A sharp interface method for two-phase compressible flows at low-Mach regime

Ziqiang Zou[1]
Surpvisor: Christian Tenaud[2] Edouard Audit[1] Nicolas Grenier[2]

[1]Maison de la Simulation, CEA, CNRS, Univ. Paris-Sud, UVSQ, Univ. Paris-Saclay, Gif-sur-Yvette, France
[2]LIMSI, CNRS, Univ. Paris-Sud, Univ. Paris-Saclay, Orsay, France

Journée Des Doctorants du LIMSI

Introduction

Flows of interest

- Compressible gas & quasi-incompressible liquid
- surface tension & heat transfer & phase change

ocean wave

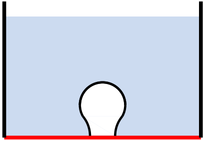

bubble growth near a heated plate

- liquid: low-Mach regime

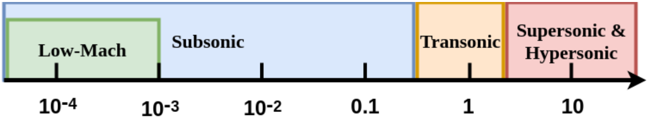

Mach number (Ma=u/c) & Flow Regimes

Introduction

Previous studies

- incompressible liquid model [Tanguy et al., 2014] [Sato and Ničeno, 2013]
  - robust, efficient
  - without compressible effects
- compressible liquid model [Fechter et al., 2017][Faccanoni et al., 2012]
  - take compressible effects into account
  - excessive numerical diffusion Error $\propto 1/Ma$
  - time step limitation $\triangle t = \triangle x/\max(c+u)$

Introduction

Previous studies

- incompressible liquid model [Tanguy et al., 2014] [Sato and Ničeno, 2013]
  - robust, efficient
  - without compressible effects
- compressible liquid model [Fechter et al., 2017][Faccanoni et al., 2012]
  - take compressible effects into account
  - excessive numerical diffusion Error $\propto 1/Ma$
  - time step limitation $\triangle t = \triangle x/\max(c+u)$

Objective

develop a compressible solver for both liquid and gas:

- Accurate at low-Mach regime
- Uniform time step with respect to the Mach number
- Well-balanced discretization of sources terms (gravity, surface tension)
- An accurate high-order method to capture the interface

Interface description

Level-Set method [Osher and Sethian, 1988]

- ϕ: signed distance function
- $|\nabla\phi| = 1$
- Normal vector $\boldsymbol{n} = \frac{\nabla\phi}{|\nabla\phi|}\Big|_{\phi=0}$
- interface Curvature $\kappa = \nabla \cdot (\frac{\nabla\phi}{|\nabla\phi|})$
- Level-Set advection $\frac{\partial\phi}{\partial t} + \boldsymbol{u} \cdot \nabla\phi = 0$

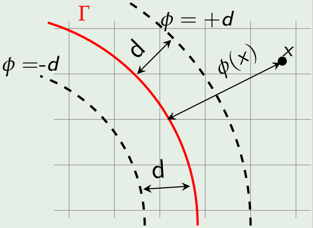

Operators splitting

Governing equations

$$\begin{cases} \partial_t \rho & +\nabla\cdot(\rho\mathbf{u}) & & =0 & & \\ \partial_t(\rho\mathbf{u}) & +\nabla\cdot(\rho\mathbf{u}\otimes\mathbf{u}) & +\nabla p & = -\rho\nabla\psi & +\nabla\cdot\boldsymbol{\tau}_{visc} & +\sigma\kappa\mathbf{n}\delta(\phi) \\ \partial_t(\rho E) & +\nabla\cdot((\rho E+p)\mathbf{u}) & & = -\rho\mathbf{u}\cdot\nabla\psi & +\nabla\cdot(\boldsymbol{\tau}_{visc}\mathbf{u}) & +\sigma\kappa\mathbf{u}\cdot\mathbf{n}\delta(\phi) \quad +\nabla\cdot(k\nabla T) \\ \partial_t\phi & +\mathbf{u}\cdot\nabla\phi & & =0 & & \end{cases}$$

$E = e + \frac{|\mathbf{u}|^2}{2}$ $\rho e = \frac{p+\gamma\pi^\infty}{\gamma-1}$ $p = \rho r T - \gamma\pi^\infty$ $r = c_p - c_v$ $\gamma = c_p/c_v$

ψ : gravitational potential $\boldsymbol{\tau}_{visc}$: viscous tensor

κ : interface Curvature k : thermal conductivity

Operators splitting

Governing equations

$$\begin{cases} \partial_t \rho & + \nabla \cdot (\rho \mathbf{u}) & & = 0 \\ \partial_t (\rho \mathbf{u}) & + \nabla \cdot (\rho \mathbf{u} \otimes \mathbf{u}) & + \nabla p & = -\rho \nabla \psi \quad + \nabla \cdot \boldsymbol{\tau}_{visc} \quad + \sigma \kappa \mathbf{n} \delta(\phi) \\ \partial_t (\rho E) & + \nabla \cdot ((\rho E + p)\mathbf{u}) & & = -\rho \mathbf{u} \cdot \nabla \psi + \nabla \cdot (\boldsymbol{\tau}_{visc} \mathbf{u}) + \sigma \kappa \mathbf{u} \cdot \mathbf{n} \delta(\phi) + \nabla \cdot (k \nabla T) \\ \partial_t \phi & + \mathbf{u} \cdot \nabla \phi & & = 0 \end{cases}$$

$E = e + \frac{|\mathbf{u}|^2}{2}$ $\rho e = \frac{p + \gamma \pi^\infty}{\gamma - 1}$ $p = \rho r T - \gamma \pi^\infty$ $r = c_p - c_v$ $\gamma = c_p / c_v$

ψ : gravitational potential $\boldsymbol{\tau}_{visc}$: viscous tensor

κ : interface Curvature k : thermal conductivity

Acoustic / Transport / Diffusion decomposition

$$\begin{cases} \partial_t \rho + \rho \nabla \cdot \mathbf{u} + \mathbf{u} \cdot \nabla \rho = 0 \\ \partial_t (\rho \mathbf{u}) + \rho \mathbf{u} \nabla \cdot \mathbf{u} + \nabla p + \mathbf{u} \cdot \nabla (\rho \mathbf{u}) = -\rho \nabla \psi + \sigma \kappa \mathbf{n} \delta(\phi) + \nabla \cdot \tau_{visc} \\ \partial_t (\rho E) + \rho E \nabla \cdot \mathbf{u} + \nabla \cdot (p \mathbf{u}) + \mathbf{u} \cdot \nabla (\rho E) = -\rho \mathbf{u} \cdot \nabla \psi + \sigma \kappa \mathbf{u} \cdot \mathbf{n} \delta(\phi) + \nabla \cdot (\tau_{visc} \mathbf{u}) + \nabla \cdot (k \nabla T) \\ \partial_t \phi + \mathbf{u} \cdot \nabla \phi = 0 \end{cases}$$

Numerical resolution

1. Acoustic system
   - perform a Suliciu-type relaxation to deal with any equation of state and obtain linearly degenerate system [Bouchut, 2004]
   - resolve the Riemann problem that takes the source term (gravity) and jump conditions related to surface tension & phase change (future work) into account in a consistent way
   - well-balanced scheme for gravity and surface tension : discretization at cell face or interface
   - low-Mach correction: the accuracy of the global scheme independent form Mach number [Chalons et al., 2016]
   - implicit scheme: $\triangle t = \triangle x / \max(|u|)$ (future work)
2. Transport system
   - sharp interface & avoid mixing cell:ghost fluid method
   - Level-Set advection: One-Step (OS) scheme [Daru and Tenaud, 2004] coupled time-space approach: same order accuracy at time & space
3. Diffusion system (viscous & heat transfer)
   - classical finite volume discretization

Numerical test

Circle advection

- advection in diagonal direction with a periodic boundary condition
- t=100 (100 periods) CFL=0.5
- local L_1 error $(|\phi| \leq 3\Delta x)$

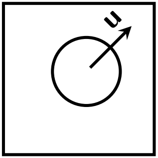

Numerical scheme

- Coupled time-space approach: high-order One-Step (OS) scheme
- Separate time-space approach: WENO-RK [Jiang and Shu, 1996]
  HOUC (High-Order upwind centered)-RK [Nourgaliev, 2007]

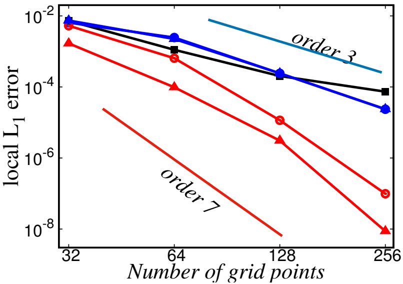

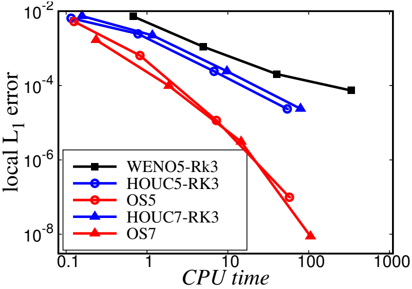

Two-dimensional sloshing [Chanteperdrix, 2004]

- $\rho_2/\rho_1 = 1000 \quad h_1/L = 1.25 \quad h_2/L = 1$
- $c_1 \approx 370m/s \quad c_2 \approx 1500m/s \quad Ma_{max} \approx 2 \times 10^{-5}$
- $a_0/g = 0.01$ resolution : $L/\Delta x = 40$

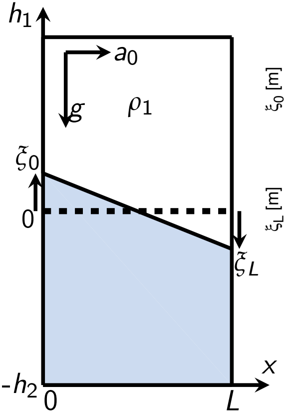

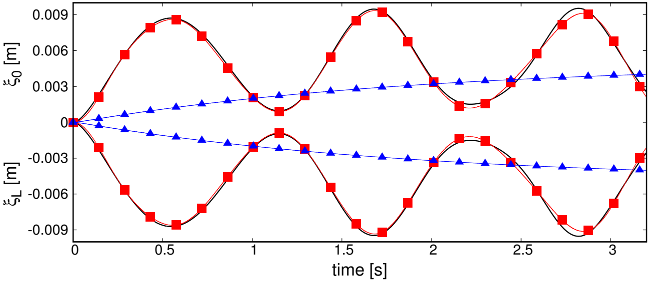

— analytical solution: linearized potential theory
■ with low-Mach correction
▲ without low-Mach correction

1D non-isothermal problem

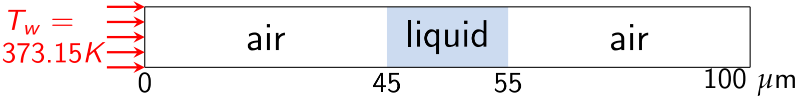

- $T_{liq} = T_{air} = 293.15K$
- liquid: $\rho = 1000kg/m^3$ $c = 1500m/s$ $c_p = 4184JK^{-1}kg^{-1}$ $k = 0.6Wm^{-1}K^{-1}$ $\mu = 1.82 \times 10^{-5}$Pa s
- air: $\rho = 1.204kg/m^3$ $c = 340m/s$ $c_p = 1004.5JK^{-1}kg^{-1}$ $k = 0.0256Wm^{-1}K^{-1}$ $\mu = 0.001$Pa s

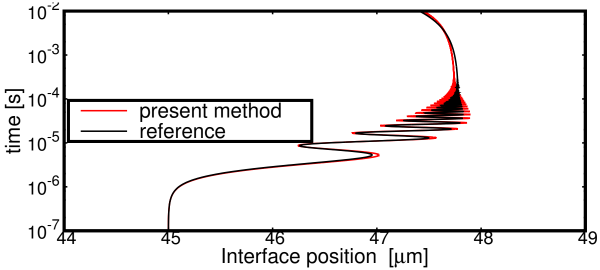

Trajectories of left interface: reference [Daru et al., 2010]

Parasitic currents

- liquid $\rho = 1 \quad c = 20 \quad p_l$
- gas $\rho = 1 \quad c = 1 \quad p_g = p_l + \sigma\kappa$

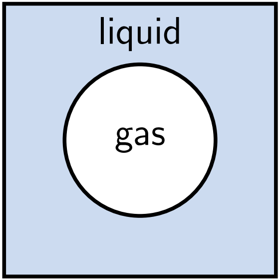

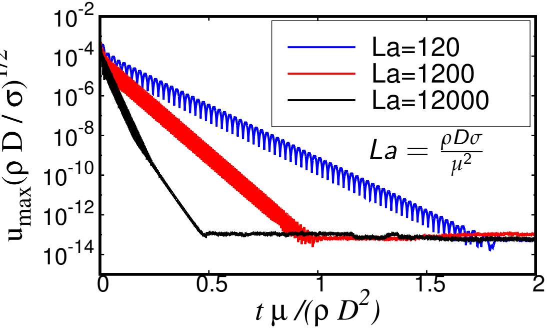

Evolution of velocity fluctuations of a 2D bubble in a slightly compressible liquid with different Laplace numbers by varying the fluid viscosity ($R = 12.8 \triangle x$)

Numerical test

Zalesak disk

- disk with a rectangular slot
- Rotating velocity field: $u = \pi(50 - y)/314 \quad v = \pi(x - 50)/314$
- one full rotation CFL=0.5

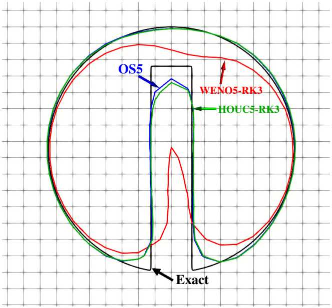

Interface representation of the Zalesak disk after one full rotation
resolution: 50×50

Rayleigh-Taylor instabilities

- $\rho_1 = 1.8 \quad \rho_2 = 1 \quad Ma_{\text{max}} \approx 10^{-2}$
- $Re = \sqrt{(H/2)^3/g}/\nu = 420 \quad Mesh: 312 \times 624$

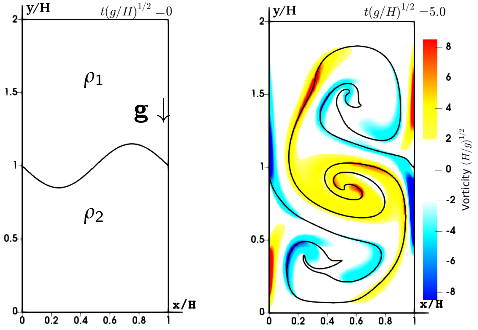

(a) (b)

Vorticity and interface representation: (a) present Level-Set formulation (b) incompressible Level-Set formulation *[Colicchio, 2004]*

Thank you for your attention !

References I

Bouchut, F. (2004).
Springer Science & Business Media.

Chalons, C., Girardin, M., and Kokh, S. (2016).
An all-regime lagrange-projection like scheme for the gas dynamics equations on unstructured meshes.
Communications in Computational Physics, 20(1):188–233.

Chanteperdrix, G. (2004).
Modélisation et Simulation Numérique des Ecoulements Diphasiques à Interfaces Libres. Application à l'étude des mouvements de liquides dans les réservoirs de véhicules spatiaux.
PhD thesis, Ecole Nationale Supérieure de l'Aéronautique et de l'Espace.

Colicchio, G. (2004).
Violent disturbance and fragmentation of free surfaces.
PhD thesis, University of Southampton, UK.

Daru, V. and Tenaud, C. (2004).
Journal of computational physics.

References II

Faccanoni, G., Kokh, S., and Allaire, G. (2012).
Modelling and simulation of liquid-vapor phase transition in compressible flows based on thermodynamical equilibrium∗.
ESAIM: Mathematical Modelling and Numerical Analysis, 46(5):1029–1054.

Fechter, S., Munz, C.-D., Rohde, C., and Zeiler, C. (2017).
A sharp interface method for compressible liquid–vapor flow with phase transition and surface tension.
Journal of Computational Physics, 336:347–374.

Jiang, G.-S. and Shu, C.-W. (1996).
Journal of computational physics.

Nourgaliev, R. R. (2007).
Journal of Computational Physics.

Osher, S. and Sethian, J. A. (1988).
Fronts propagating with curvature-dependent speed: algorithms based on hamilton-jacobi formulations.
Journal of computational physics, 79(1):12–49.

References III

Sato, Y. and Ničeno, B. (2013).
A sharp-interface phase change model for a mass-conservative interface tracking method.
Journal of Computational Physics, 249:127–161.

Tanguy, S., Sagan, M., Lalanne, B., Couderc, F., and Colin, C. (2014).
Benchmarks and numerical methods for the simulation of boiling flows.
Journal of Computational Physics, 264:1–22.